

Seasonal variation of heat-storage in the tropical Atlantic Ocean

Heat-storage
Atlantic
Tropic
Seasonal variation
Climate
Contenu thermique
Atlantique
Tropique
Variation saisonnière
Climat

J. Merle

CIMAS, 4600 Rickenbacker causeway, Miami, Florida 33149, USA.

ORSTOM, 24 rue Bayard, 75008 Paris.

Present affiliation : Laboratoire d'Océanographie Physique du Muséum National d'Histoire Naturelle, 43 rue Cuvier. 75231 Paris Cedex 05.

Received 6/2/80, in revised form 25/4/80, accepted 10/5/80.

ABSTRACT

The monthly mean heat-content in the superficial (0-300 m) layers of the tropical Atlantic Ocean (20°N-20°S) is obtained through the processing of all available Nansen historical data.

Large, non-symmetrical in relation to the equator, spatial variations are observed. It is the depths' repartition of the thermocline which fits in best with the spatial repartition of heat-content. Seasonal variations of heat-content are large, especially in the equatorial band. These variations are due to a seasonal uplifting of the thermocline. An Eastward movement of the annual heat-content signal's phase, along the equator, suggests a baroclinic event affecting the whole thermocline on a seasonal time-scale.

The local seasonal variations of heat-content in the equatorial region are found to be about 10 times larger than the seasonal variations of the oceanic heat-gain from the atmosphere through the surface. Thus, the ocean dynamics, more than the local thermal forcing by the atmosphere, is responsible for the seasonal variations of heat-content in the upper layers (0-300 m) of the tropical Atlantic Ocean. This huge redistribution of heat by the ocean circulation on a seasonal time-scale, could explain the singularities noticed by Oort and Vonder Haar (1976) in the low latitudes concerning the out of phase of the heat-storage seasonal variation and the large cross-equatorial meridional heat-fluxes found for the whole North hemisphere.

Oceanol. Acta, 1980, 3, 4, 455-463.

RÉSUMÉ

Variation saisonnière du contenu thermique dans l'océan Atlantique tropical

Le contenu thermique des couches superficielles (0-300 m) de l'océan Atlantique intertropical (20°N-20°S) est calculé par moyenne mensuelle en utilisant l'ensemble des données historiques disponibles de type Nansen.

Des variations spatiales importantes, non symétriques par rapport à l'équateur, sont observées. Il apparaît que c'est la profondeur de la thermocline qui caractérise le mieux les variations spatiales du contenu thermique. Les variations saisonnières du contenu thermique sont très importantes, particulièrement dans la bande équatoriale. Ces variations sont dues à des mouvements verticaux de la thermocline, et un déplacement progressif d'Ouest en Est de la phase du signal annuel du contenu thermique au voisinage de l'équateur suggère qu'un mouvement baroclinique affecte cette thermocline à une échelle saisonnière.

La comparaison du taux de variation mensuelle du contenu thermique avec les valeurs mensuelles du gain thermique océanique à travers sa surface, montre que les variations saisonnières du contenu thermique sont d'un ordre de grandeur 10 fois supérieur au gain net de chaleur par l'océan. C'est donc la dynamique océanique, plus que l'action

O.R.S.T.O.M. Fonds Documentaire

N° : 18
Cote : B

thermodynamique locale de l'atmosphère, qui conditionne les variations saisonnières du contenu thermique des couches superficielles (0-300 m) de l'océan Atlantique tropical. Ce sont ces redistributions thermiques considérables opérées par la circulation océanique qui peuvent expliquer les singularités observées pour l'ensemble de l'hémisphère Nord par Oort et Vonder Haar (1976) concernant le déphasage de la variation saisonnière du taux de stockage thermique aux basses latitudes et les flux méridiens transéquatoriaux.

Oceanol. Acta, 1980, 3, 4, 455-463.

INTRODUCTION

Heat-storage and heat-transport are the most important functions of the ocean in the climate. Recent investigations have focused attention on the large meridional oceanic heat-transport occurring at low latitudes in the entire North hemisphere (Oort, Vonder Haar, 1976). Strong seasonal variations and out of phase in the rate of heat-storage in tropical oceans suggest a zonal redistribution of heat by equatorial oceanic currents on a seasonal time-scale (Fig. 1). Heat-fluxes through the oceanic surface have also been recently estimated by several authors (Hastenrath, Lamb, 1978; Bunker, Worthington, 1976), using historical sea surface observations. Large seasonal variations are also found in tropical oceans.

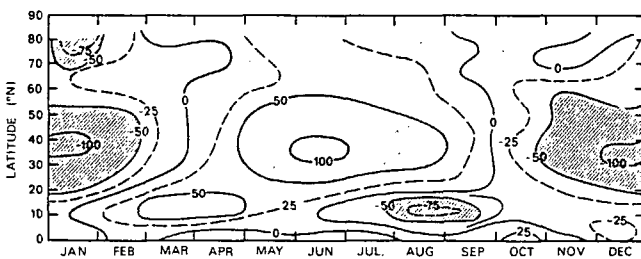


Figure 1
Rate of heat storage in the oceans of the North hemisphere (in W/m^2).
From Oort and Vonder Haar (1976).
Taux de variation du contenu thermique dans les océans de l'hémisphère Nord (en W/m^2), d'après Oort et Vonder Haar (1976).

In the tropical Atlantic Ocean, the number of hydrographic observations allow one to reasonably estimate some aspects of the seasonal variation of the heat-content. We use the basic law of the energy conservation for the water column

$$F_H = \text{DIV}(\vec{T}_H) + \Delta HS \tag{1}$$

with F_H , the net flux of heat through the air-ocean interface:

\vec{T}_H , the oceanic heat-transport;

ΔHS , the rate of oceanic heat-storage. The divergence of the heat-transport can be obtained as a residual term knowing F_H and ΔHS .

The purpose of this study is to describe the seasonal variation of the heat-content in the tropical Atlantic Ocean. Using the above relation, divergence of heat-transport is also investigated, and some information of the seasonal variation of the heat-transport is inferred.

DATA AND PROCESSING

The data used in this study belong to the Nansen data file archived by the NODC. About 18 000 hydrographic casts are considered in the 30°N-30°S band. Most of them (10 000) are concentrated in the 10°N-10°S band. Due to this unequal spatial partition of data, we consider two scales of processing: a global scale zonally integrating data in large latitudinal bands (5° at least), and a more detailed scale in the near equatorial area distinguishing East and West regions by smaller latitudinal bands (2°; see Fig. 2). For a global distribution of data, see Merle (1978). A screening routine has been applied using the T-S relation in squares of 5 × 5°, and for each trimester. Suspicious stations appear clearly in the central waters where the T.S relation is linear. About 15% of the data have been rejected. Data have been grouped by squares of 2° latitude by 4° longitude, and monthly. The linear interpolation at standard levels and mean in each of the 2 × 4° boxes, have been processed. Missing data in some boxes and for some months, have been interpolated from adjacent boxes and months.

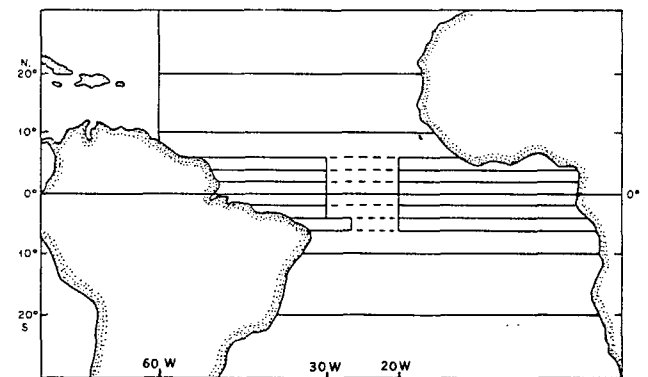


Figure 2
Location of the areas considered in the study.
Carte de situation des régions étudiées.

The relative heat-content around a depth Z_N and with reference to 0°C, is calculated by:

$$HS(Z_N) = \frac{1}{10} \overline{JDC}_p \sum_{i=1}^N (T_i - T_{i-1})(Z_i - Z_{i-1})$$

with T_i , the temperature at each standard level in C degrees;

Z_i , the depth of standard levels in meters;

C_p , the heat capacity of sea-water;

\overline{JDC}_p , the mean density of the water column.

\overline{JDC}_p has been taken equal to 0.4096. Then $HS(Z_N)$ is given in Joule per square meter. In the most part of this

study $Z_N = 300$ m. The rate of heat-storage ΔHS for a given month, is obtained through the difference of heat-content between two adjacent months. For example, $\Delta HS_{July} = (HS_{August} - HS_{June})/2$; ΔHS is converted to watt per square meter.

Standard deviations of heat-content from the surface down to 300 m, are generally large, of the order of $2 J/m^2$, and in some areas the small number of data gives a relatively low significance in terms of the confidence interval. But the consistency of the results presented in the following sections, represents a good test of the global significance of these results.

RESULTS

Mean annual heat-storage pattern

Large spatial variations of the mean annual heat-content from the surface down to 300 m, are observed in the tropical Atlantic Ocean; the range of values appears from $160 J/m^2$ off the African coast at $20^\circ S$, to $270 J/m^2$ at $20^\circ N$ and $60^\circ W$ (Fig. 3). Lower values are found in the Eastern regions ($< 200 J/m^2$). Strong zonal gradients appear in the vicinity of $20^\circ N$ and $20^\circ S$. Near equatorial areas on the contrary, are affected by a weaker zonal gradient. North of the equator ($3-5^\circ N$), a ridge of relative maximum values appears at the Southern border of the

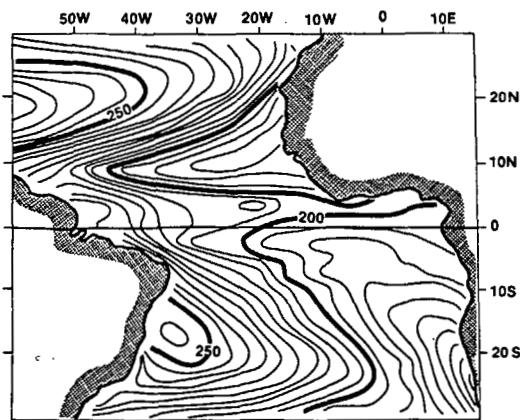


Figure 3
Distribution of heat-content from 0 to 300 m-depth in the tropical Atlantic Ocean. Units are Joules per square meter.
Moyenne annuelle du contenu thermique entre 0 et 300 m dans l'Océan tropical Atlantique. L'unité est le Joule par mètre carré.

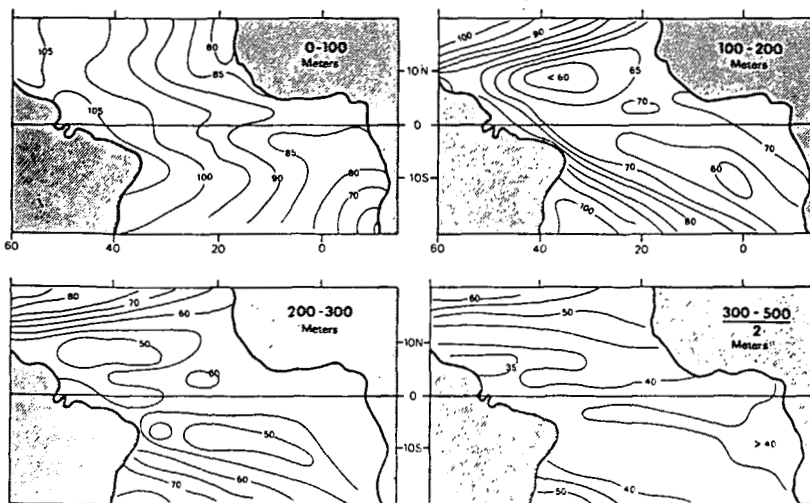


Figure 4
Repartition of heat content (J/m^2) from 0 to 500 m-depth by layers of 100 m. Note that from 100 to 300 m-depth (thermocline), the largest spatial variations are observed.

Moyenne annuelle du contenu thermique entre 0 et 500 m par tranches de 100 m. Remarquez que c'est entre 100 et 300 m (profondeur de la thermocline) que les variations spatiales du contenu thermique sont les plus importantes.

North Equatorial Counter-Current. The subsurface layers, from 100 to 300 m, which roughly belong to the main thermocline, appear to be responsible for this global pattern of the mean annual heat-content (Fig. 4); the largest spatial variations are observed in the 100 to 200 m layer. Hence, the spatial variation of the 0 to 300 m heat-content layer, is mainly related to the spatial variation of the depth of the thermocline, and appears to be very different from the mean sea-surface temperature-pattern. Thus, the zonal gradient of heat-content appears to be mainly due to the zonal slope of the thermocline (Merle, 1980).

Seasonal variations of heat-storage

Seasonal variations of heat-content are not confined to the mixed layer; the thermocline-layer has to be accounted for. As an example, Merle (1980) showed that in the equatorial band, subsurface layers down to 300 m are affected by seasonal variations. This fact justifies the integration of heat-content down to 300 m, in order to fully describe its seasonal variations. Phase-differences between the surface layer (0-50 m) and subsurface layers, are also observed. These phase-differences seem to affect only the Western regions (from the Brazilian coast to $32^\circ W$), where the mixed layer is very thick (Fig. 5 a and 5 b). This phase-change in the near equatorial band ($2^\circ N-2^\circ S$), will be discussed in detail. Unfortunately, on the outside of the equatorial band, data are so scarce that it is not possible to investigate any zonal change in the annual signal of heat-storage. We will consider only these regions zonally in averaging heat-content in large zonal bands of several degrees of latitude, corresponding approximately to the major components of the equatorial current system.

If we consider the $20^\circ N-20^\circ S$ intertropical region as a whole, the annual signal of heat-storage from 0 to 300 m appears to be minimal during the Southern Summer (June to August), and maximal during the Southern Spring (November-December): Figure 6 a. The amplitude of the annual variation is about $3 J/m^2$. Separating each hemispheric part of this region, it appears that the Southern tropical region ($0-20^\circ S$) is also characterised by a minimum of the heat-storage annual signal in the Winter season (June to September). The maximum appears in Summer (December to March). The amplitude

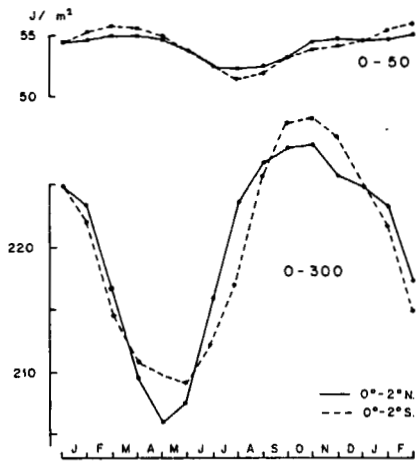


Figure 5a
Seasonal variation of heat-content in the 0-50 and 0-300 m layers, and for the 0-2°N and 0-2°S Western equatorial bands. See Figure 2.

Variation saisonnière du contenu thermique entre 0 et 50 m et entre 0 et 300 m pour les bandes 0-2°N et 0-2°S de la région Ouest (voir fig. 2).

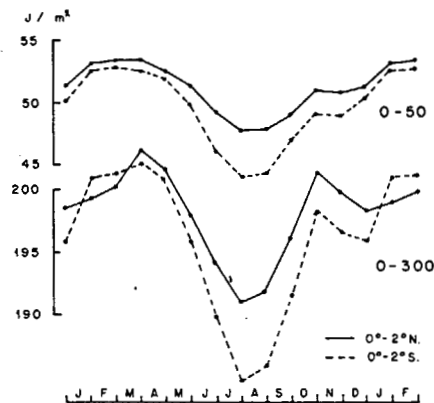


Figure 5b
Same as 5a, for the Eastern (0-2°N and 0-2°S) equatorial bands (Gulf of Guinea). See Figure 2.

Semblable à 5a, mais pour la région Est (voir fig. 2).

is about 5 J/m^2 . The Northern tropical region ($0-20^\circ\text{N}$) does not show any typical Northern aspect. If a marked minimum is observed in the Northern Winter (January to April), a Summer maximum does not clearly appear; it seems that the two periods of maxima, in Spring (June-July) and fall (October-December), can be distinguished; a secondary minimum in August could be due to the influence of the Southern minimum in this season. Thus the annual signal of the global region ($20^\circ\text{N}-20^\circ\text{S}$) seems almost in phase with its Southern component, suggesting a predominant influence of the Southern hemisphere.

Considering the $10^\circ\text{N}-10^\circ\text{S}$ region as a whole (Fig. 6b), its annual cycle of 0-300m heat-content shows also a minimum from June to September and a maximum in November-January, similar to that observed in the $20^\circ\text{N}-20^\circ\text{S}$ region. Nevertheless, the $10^\circ\text{N}-10^\circ\text{S}$ region shows a

larger amplitude (5 J/m^2), suggesting an amplification of the annual signal in the near equatorial regions. This point will be discussed further on. Considering each hemisphere, the Northern region ($0-10^\circ\text{N}$) has a pattern similar to that of the $0-20^\circ\text{S}$ region with a maximum in the fall and early Winter (October-December) and a minimum in the late Winter (February-April). The Southern region ($0-10^\circ\text{S}$) is also similar to the $0-20^\circ\text{S}$ region with a marked minimum in the Northern Summer (July-September), and a maximum extending during all the Winter, from November to April. It is clear that the annual cycle of heat-content of the $10^\circ\text{N}-10^\circ\text{S}$ region is mainly in phase with its Southern region ($0-10^\circ\text{S}$), and therefore that the equatorial Atlantic area is essentially thermally governed by the Southern hemisphere. Figure 3 suggests that from 20°N to 20°S , we can distinguish different zonal bands in relation with the main major currents of the equatorial system. Outside of the equatorial band ($6^\circ\text{N}-6^\circ\text{S}$), investigated in the next paragraph, we will consider a $6^\circ\text{N}-10^\circ\text{N}$ region, or North Equatorial Counter-Current (NECC) region; a $10^\circ\text{N}-20^\circ\text{N}$ region, or North Equatorial Current (NEC) region; a $6^\circ\text{S}-10^\circ\text{S}$ region (Fig. 7).

Figure 7
Seasonal variation of heat-content for various zonally averaged bands from 20°N to 10°S .

Variation saisonnière du contenu thermique pour différentes bandes zonales entre 20°N et 10°S .

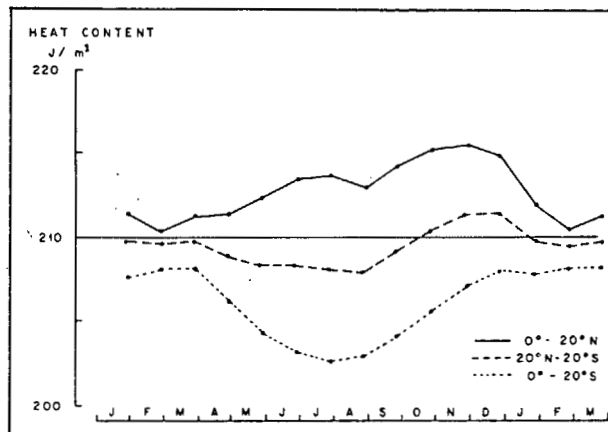
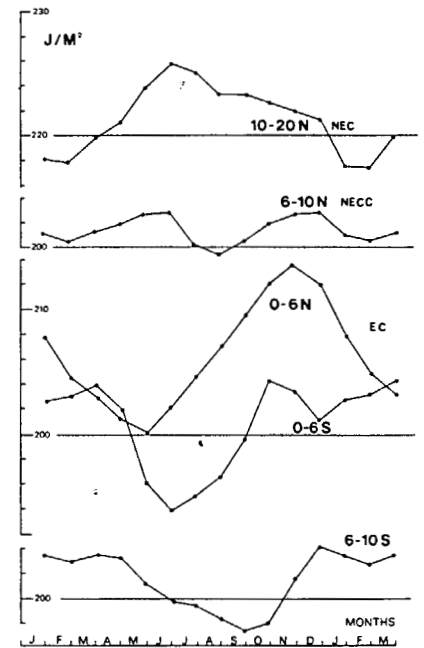


Figure 6a
Seasonal variation of heat-content from 20°N to 20°S .
Variation saisonnière du contenu thermique entre 20°N et 20°S .

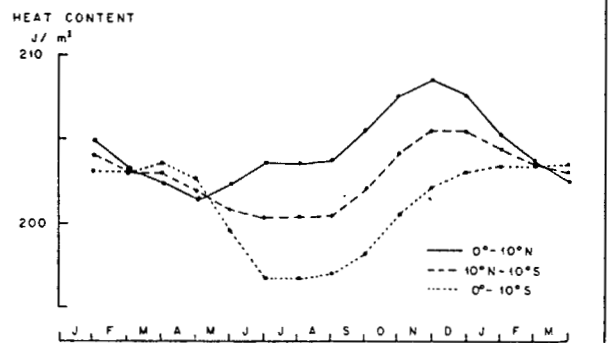


Figure 6b
Same as 6a, for $10^\circ\text{N}-10^\circ\text{S}$.
Semblable à 6a, mais entre 10°N et 10°S .

The NEC region (10°N - 20°N) shows a typical North tropical pattern with a marked maximum in Summer (June-September) and a minimum in Winter (December-March), but few data are available in this region, and standard deviation for each monthly mean is about 2 J/m^2 ; therefore, a weak confidence can be given to the details of this annual variation. The 6°N - 10°N region (NECC) is characterized by a bimodal annual cycle with two marked maxima in Northern Spring (May-June) and fall (November-December), suggesting an alternative influence of the Northern and Southern hemisphere. A similar annual cycle of the Sea Surface Temperature (SST) has been observed in this region (Merle, Fioux, Hisard, 1979). Compared to this large semi-annual component of the signal, the annual amplitude appears minimal. The symmetrical Southern region (6°S - 10°S) shows a larger amplitude than the Northern region, with a marked minimum in the Northern Summer (July-September), and a long period of maxima with possibly, as for the Northern region, a bimodal cycle. But in this region also the poor density of data give only a limited confidence in the detail of these results.

Particular attention should be devoted to the equatorial region (6°N - 6°S) where, fortunately, the density of data allows a more detailed investigation. Comparatively to the other regions described above, the equatorial region is characterized by a large amplitude of the heat-content annual cycle, both for its Northern (0 - 6°N) and Southern (0 - 6°S) parts. A preliminary study of this equatorial region (Merle, 1980) has focussed attention on the important difference which exists between the Eastern equatorial region (Gulf of Guinea) and the Western equatorial region. Figures 8a and 8b present the annual cycle of the heat-content from 0 to 300 m by 2° latitudinal band, and for the Western and Eastern equatorial regions (for a precise localisation of these regions, see Fig. 2). In the Western region, the amplitude of this 0-300 heat-

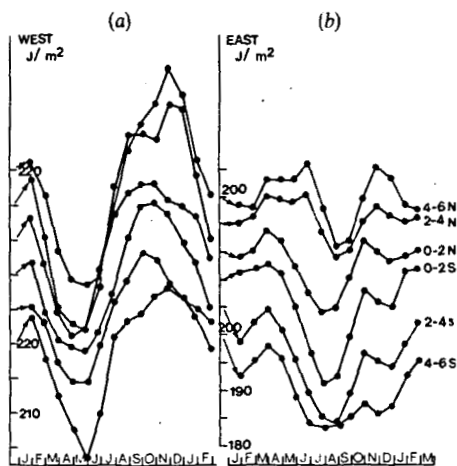


Figure 8a

Seasonal variation of heat-content (J/m^2) from 0 to 300 m in boxes of 2° latitude from 6°N to 6°S , and in the Western region of the equatorial Atlantic (see Fig. 2). Curves are shifted equal distances. From Merle (1980).

Variation saisonnière du contenu thermique entre 0 et 300 m dans des bandes zonales de deux degrés de latitude entre 6°N et 6°S pour la région Ouest (voir fig. 2), d'après Merle (1980).

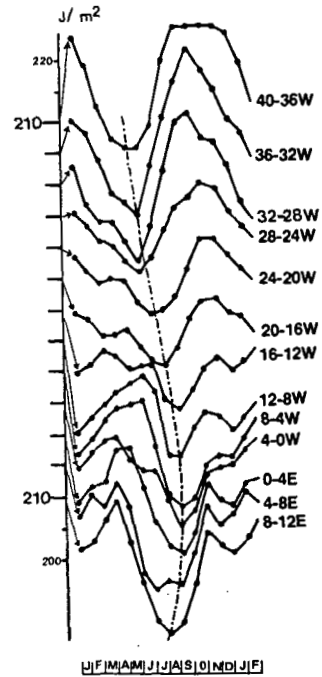
Figure 8b

Same as 8a, for the Eastern region (Gulf of Guinea).
Semblable à 8a pour la région Est (Golfe de Guinée).

Figure 9

Annual variation of the heat-content (0 - 300 m) (J/m^2) along the equatorial region (from 4°N to 4°S) averaged by 4° longitude. The minimum is indicated by a dotted line. Note the continuous Eastward phase displacement from the Western region to the 0 - 8°W region. From Merle (1980).

Variation saisonnière du contenu thermique entre 0 et 300 m le long de l'équateur (de 4°N à 4°S) et par 4° de longitude. Le minimum est marqué par un trait pointillé. Remarquer le changement de phase continu depuis l'Ouest jusqu'à environ 8°W . D'après Merle (1980).



content annual cycle is about twice larger than in the Eastern region, and important phase-differences are observed. In order to determine if these phase-changes can be followed continuously along the equator, the region has been divided into boxes of 4° -longitude and 8° -latitude (4°N - 4°S), from 50°W to 12°E . Figure 9 shows a continuous phase-variation, suggesting an Eastward propagation from 50°W to about 5°W , and further East (from about 5°W to the African coast), on the contrary a Westward propagation.

We should note that the SST annual variation studied by Merle *et al.* (1979) shows a different feature. SST annual amplitude variation is maximal in the Eastern Atlantic equatorial ocean, and about five times larger than in the Western equatorial region. But the phase-propagation of this SST signal has also been found Westwards, in the Gulf of Guinea (Merle, Le Floch, 1978). The apparent contradiction between amplitude of variation of heat-content and SST can be easily explained in considering the annual variation of the structure and depth of the thermocline. The equatorial section of the mean annual temperature-field, from 2°N to 2°S and from 50°W to 15°E (African coast), shows a general Eastward slope of the thermocline, from about 100 m in the West to about 20 m at about 5°W ; and a large seasonal variation of this thermocline-depth can be noted, especially in the West, where the range of depth-variation of the 23°C isotherm appears to be between about 150 and 75 m (Merle, 1980). Then, it seems clear that the observed, large seasonal variation of the heat-content from the surface down to 300 m in the Western equatorial region, is due to the seasonal uplifting of the thermocline, which does not affect the SST. In the Eastern equatorial region on the contrary, the smaller amplitude of the seasonal heat-content variation is due to the smaller range of the depth-variation of the thermocline, which is near the surface. The seasonal near surfacing of this thermocline, explains the large amplitude of the seasonal variations of the SST.

The similarity of the Westward phase propagation of the annual signal of heat-content and SST in the Eastern

equatorial Atlantic (Gulf of Guinea), is also due to this near surfacing of the thermocline, whose depth variation affects both heat-content and SST. In the Western and Central region, the Westward propagation of the annual signal of heat-content cannot be related to a propagation of the annual signal of SST, because this signal becomes very small and no clear propagation can be depicted.

Seasonal variations of rates of heat-storage and heat-divergence

The difference in heat-content from month to month gives the rate of heat-storage ΔHS (gain or loss). According to Equation (1)

$$\text{DIV}(\vec{T}_H) = F_H - \Delta HS.$$

The annual progress of F_H is provided by Hastenrath and Lamb (1976) for some selected regions in the Western and Eastern equatorial Atlantic ocean. Using these data, we obtain an estimate of the seasonal variation of the oceanic heat-divergence.

The whole intertropical region 20°N-20°S, is characterized by a period of heat-divergence (export) during the first semester (from December to June), but a convergence of heat (import) seems to occur from September to November (Fig. 10 a). For each hemispheric part (0-20°N and 0-20°S) of this global intertropical region, the seasonal variation of the net oceanic heat-gain provided by Hastenrath and Lamb, has a similar amplitude to that of the seasonal variation of the rate of heat-storage, but phases do not fit. If we consider the 10°N-10°S band, the amplitude of the seasonal variation of the rate of heat-storage increases and appears some three times larger than the amplitude of the seasonal variation of the net heat-gain through the surface (Fig. 10 b). This 10°N-10°S region as a whole, is

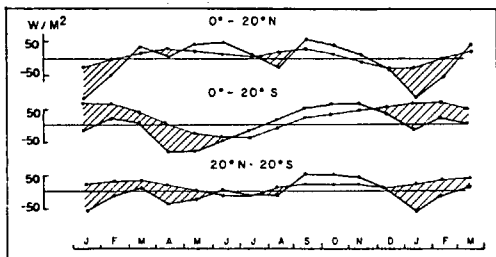


Figure 10 a
Seasonal variation of rate of heat storage and net ocean heat gain, from Hastenrath and Lamb (1978). From 20°N to 20°S. Units are watts per square meter. Dashed areas represent oceanic divergence of heat (heat export).

Variation saisonnière entre 20°N et 20°S du taux de stockage thermique et du bilan énergétique net à l'interface, d'après Hastenrath et Lamb (1978). Les zones hachurées représentent une divergence de chaleur.

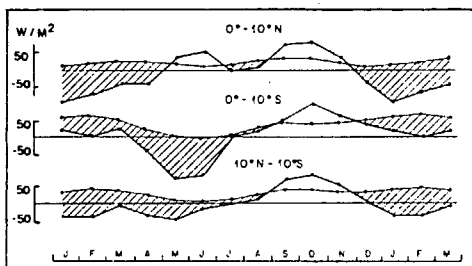


Figure 10 b
Same as 10 a, but from 10°N to 10°S.
Semblable à 10 a. mais pour 10°N-10°S.

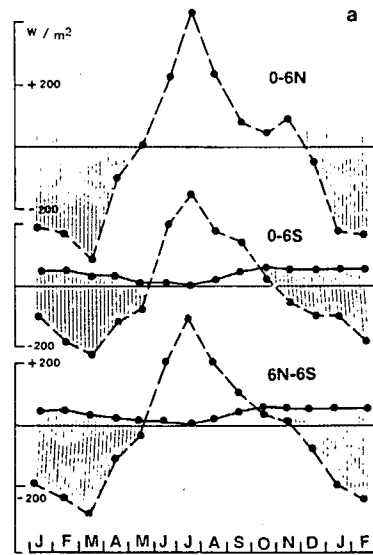


Figure 11 a
Seasonal variation of rate of heat storage (dotted line) and net heat oceanic gain (full line) in the Western equatorial Atlantic region: 0-6°N, 0-6°S and 6°N-6°S regions are considered. The values of net heat gain are provided by Hastenrath and Lamb (1978) for the region of 0-5°S only. We assume that these values are representative of the 0-6°S and 0-6°N region considered here. From Merle (1980).

Variation saisonnière du taux de stockage thermique (tiretés) et du bilan énergétique net à l'interface (trait plein) dans la région Ouest entre 6°N et 6°S. Les valeurs du bilan énergétique net sont fournies par Hastenrath et Lamb (1978) pour la région 0-5°S. On considère que ces valeurs sont représentatives de l'ensemble de la région 6°N-6°S, d'après Merle (1980).

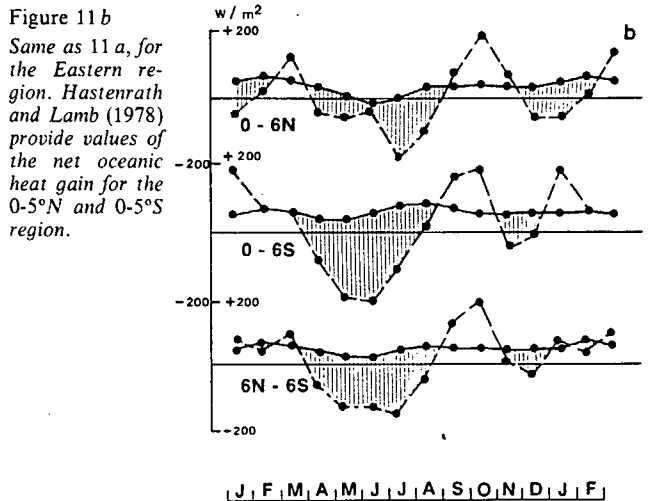


Figure 11 b
Same as 11 a, for the Eastern region. Hastenrath and Lamb (1978) provide values of the net oceanic heat gain for the 0-5°N and 0-5°S region.

Semblable à 11 a pour la région Est. Hastenrath et Lamb (1978) donnent les valeurs du bilan énergétique net à l'interface pour les régions 0-5°N et 0-5°S.

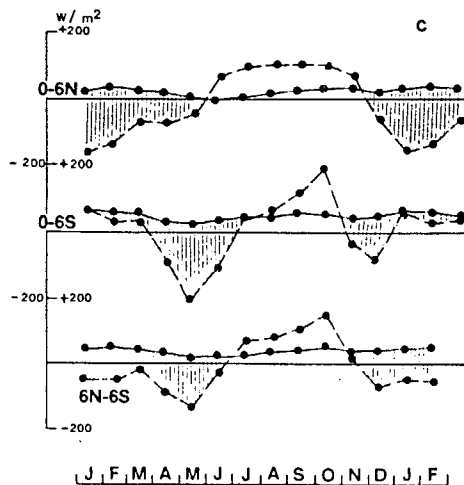


Figure 11 c
Same as 11 a, for the entire zonal Atlantic bands. The values of net heat gain are those provided by Hastenrath and Lamb (1978) for the 0-5°N, 0-5°S and 5°N-5°S bands.
Semblable à 11 a pour l'ensemble de la bande zonale Atlantique.

exporting heat during the major part of the year, except in the fall from September to December. Distinguishing each hemisphere, the Southern region (0-10°S) is exporting heat with a maximum in Spring (from April to June), and importing heat in the fall (from September to November). The Northern region (0-10°N) is exporting heat mainly in Winter (from December to April), but it seems that there are two periods of import of heat: a fall main period (September to November), and a secondary period in Spring (April to June).

In the near equatorial band (6°N-6°S), the seasonal variation of the rate of heat-storage appears even larger; its amplitude is found some eight times larger than the amplitude of seasonal variations of the net heat flux through the surface (Fig. 11 a, b, c). Heat-export is observed year round, but from July to October. Northern (0-6°N) and Southern (0-6°S) regions are slightly different in phase, showing a maximum of heat-export in January in the Northern region, and in May in the Southern region. We can also note in the Southern region a secondary maximum of heat-export in December. In this 6°N-6°S band, changes in amplitude and in phase by 2° latitude from 6°N to 6°S, appear to be continuous and consistent (Fig. 12). Nevertheless, important differences

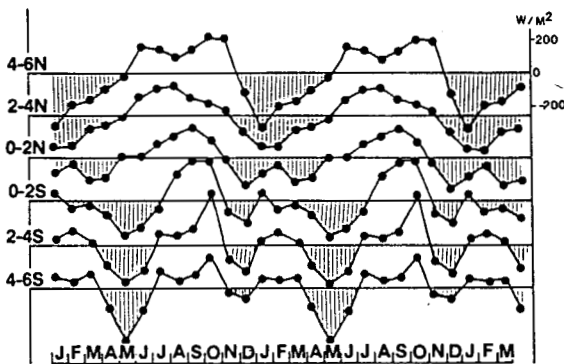


Figure 12
Seasonal variation of rate of heat storage by 2° latitude band from 6°N to 6°S. Units are watts per square meter. Note the continuous evolution of curves from North to South.

Variation saisonnière du taux de stockage thermique par 2° de latitude de 6°N à 6°S. L'unité est le watt par mètre carré. Remarquez l'évolution continue des courbes du Nord au Sud.

between Eastern and Western regions can be noted. In the Western region (from the Brazilian coast to 32°W, Fig. 11 a), the annual cycle of the rate of heat-storage is unimodal with a marked maximum in July and a minimum in March. No significant difference could be noted between the North (0-6°N) and the South (0-6°S). In the Eastern region (Gulf of Guinea, Fig. 11 b), the annual cycle of the rate of heat-storage appears bimodal, giving two periods of heat-export. The main period takes place from April to August. The secondary period appears in November-December. Differences between the North (0-6°N) and the South (0-6°S) are noticeable. It seems that the heat-export of the total region (6°N-6°S) is mainly due to its Southern part (0-6°S), and the secondary period of heat-export is more marked and appears earlier in the Northern region (0-6°N).

DISCUSSION AND CONCLUSIONS

The intertropical oceanic regions are providing the heat necessary to equilibrate the heat-losses of the middle and high latitudes. On a long-term mean (annual), we can assume that the oceanic heat-content does not vary, and equation (1) becomes:

$$F_H = \text{DIV}(\vec{T}_H)$$

The divergence of the oceanic heat-transport is equal to the net heat-gain by the ocean. Several papers in the past gave an estimate of this divergence of the mean oceanic heat-transport zonally integrated by latitude for the World Ocean (Sverdrup, 1957; Budyko, 1956; Bryan, 1962; Vonder Haar, Oort, 1973). All these authors found a large maximum near the equator and positive values covering the intertropical regions. In the Atlantic Ocean, Emig (1967), using the Budyko data, and Hastenrath (1977), using a different and more complete data set, found a similar result (Fig. 13).

But this region of the maximum mean heat-divergence is affected by seasonal variations. Oort and Vonder Haar (1976) found that these are very large and even maximal in the tropics. Negative values of heat-divergence can even be observed in some seasons near the equator.

The seasonal variation of heat-divergence is caused by two factors:

1° seasonal variation of heat-storage (HS); 2° seasonal variations of net heat-gain (F_H). The main result of our study is that the seasonal variation of heat-storage (ΔHS : rate of heat-storage) is the most important factor affecting the seasonal variation of heat-divergence in the intertropical Atlantic Ocean. In the whole intertropical region (20°N-20°S), the amplitude of the seasonal variation of ΔHS is about twice the amplitude of the seasonal variation of F_H (Fig. 10 a). But if we consider smaller regions, this ratio is increasing, due to the fact that the larger the area, the most effective the compensation between the different values (negative or

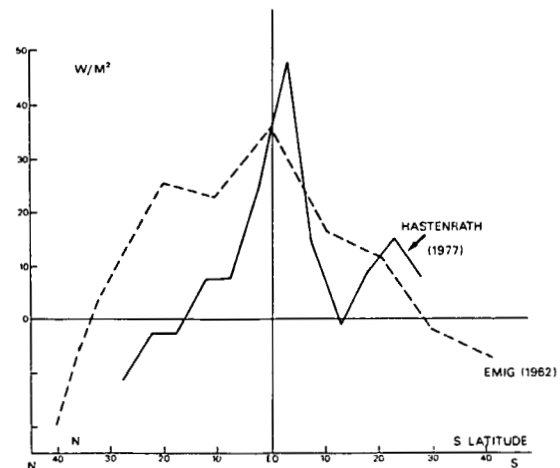


Figure 13
Latitudinal variation of mean annual oceanic heat divergence ($\text{DIV}(\vec{T}_H)$) in the tropical Atlantic Ocean. From Hastenrath (1977) and Emig (1962).
Variation en fonction de la latitude de la moyenne annuelle de la divergence océanique ($\text{DIV}(\vec{T}_H)$) dans l'Océan Atlantique tropical, d'après Hastenrath (1977) et Emig (1962).

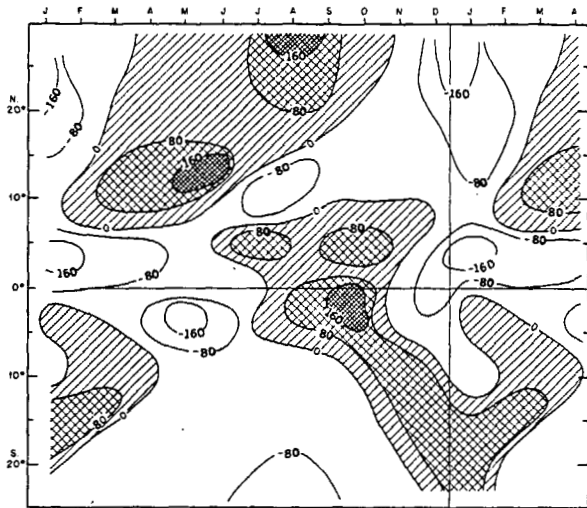


Figure 14
Seasonal and latitudinal variation of rate of heat storage (ΔHS) in the tropical Atlantic Ocean. Units are watts per square meter. Dashed areas represent positive values or increasing values of the heat-content. Note the similarities with the Oort-Vonder Haar diagram (Fig. 1), particularly the phase-difference of the period of heat-storage's positive rate around $10^\circ N$ (in Spring).

Diagramme temps-latitude des variations du taux de stockage thermique (ΔHS) dans l'Océan Atlantique tropical. L'unité est le watt par mètre carré. Les zones hachurées représentent un accroissement du stockage thermique. Remarquez la similitude avec la figure 1 de Oort et Vonder Haar, particulièrement en ce qui concerne le déphasage de la période d'accroissement maximal du stockage thermique autour de $10^\circ N$ (printemps).

positive) of smaller included areas. Thus, in the $10^\circ N$ - $10^\circ S$ region, the amplitude of the seasonal variation of ΔHS is about three to four times higher than the amplitude of the seasonal variation of F_H (Fig. 10 b). The monthly variation of the zonal integration by 5° latitude-bands of ΔHS (Fig. 14), can be compared with similar graphs provided by Hastenrath (1977) for F_H (Fig. 15). It appears that the F_H values are about 1/4 of the ΔHS values. But this zonal integration is strongly smoothing the ΔHS values because, as we saw in the equatorial region at least, large zonal changes both in amplitude and phase of the annual signal of HS, are observed (Fig. 8, 9 and 11). For example, in the Western region of the $6^\circ N$ - $6^\circ S$ band, the ratio of the amplitude of seasonal variations of ΔHS and F_H , is about 10 (Fig. 11 b). All the regions here considered, show also an important phase-difference between seasonal variations of ΔHS and F_H . Thus, the difference $\Delta HS - F_H$ representing the heat-divergence, also has a large amplitude of seasonal variations and can even change sign. It seems that such is the case in the fall (September to December) in the global $20^\circ N$ - $20^\circ S$ region (Fig. 10 a). Where does this heat come from during this season? From the North, or from the South? We can only make some speculations, since we cannot compute the meridional component of the heat-flux vector from its divergence without a zonal boundary. We may suppose that this heat is coming from the North because in the fall, the heat-content in the Northern hemisphere is maximal. Emig (1967) did the computation of the meridional component of heat-flux in the three oceans, using Budyko's (1956) data. In the Atlantic Ocean, he found that in the Tropics, the mean annual heat-transport is Northward. Thus, we can suppose that this Northward flow appears during the period of the

year when the $20^\circ N$ - $20^\circ S$ region is exporting heat (positive divergence), mainly in Winter and Spring (December to July-August); and consequently, that during the period of heat-import, the heat-flow is Southward, and coming from the North.

This Northward mean heat-flow is certainly related to the thermal intertropical mean structure observed (Fig. 3). We already noticed that the 0 - $10^\circ N$ and even the 0 - $20^\circ N$ regions as a whole, are influenced by the Southern hemisphere, as appears in the curves of the seasonal variations of heat-content (Fig. 6 a and 6 b). We should also remark that the equator is not an axis of symmetry: a maximum of heat-content appears at about $3^\circ N$ and a minimum at about $10^\circ N$ and $3^\circ S$, suggesting that the entire equatorial system is shifted of about 3° toward the North, with a real thermal equator at about $3^\circ N$. This thermal equator is lying under the mean position of the atmospheric Inter-Tropical Convergence Zone (ITCZ), and is characterized by a maximum of the sea-surface temperature (Hastenrath, Lamb, 1978; Lamb, 1978), and a minimum of the amplitude of the SST seasonal variations (Merle, Le Floch', 1978). This region is also the Southern boundary of the NECC, which is probably, as in the Pacific Ocean, advecting a large quantity of heat toward the East. The rôle of this warm advection has been invoked to explain a "El Niño"-like phenomenon in the Eastern equatorial Atlantic (Merle, Fioux, Hisard, 1979; Hisard, Merle, 1979). Zonal advection certainly plays a very important rôle in the near equatorial regions.

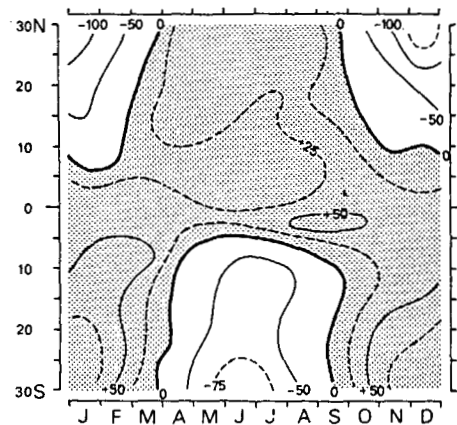


Figure 15
Seasonal and latitudinal variation of net heat gain (F_H) in the intertropical Atlantic Ocean. Units are watts per square meter. From Hastenrath (1977).

Diagramme temps-latitude du bilan énergétique net à l'interface (F_H) dans l'Atlantique tropical. L'unité est le watt par mètre carré. D'après Hastenrath (1977).

The phase-displacement of 3-4 months from West ($50^\circ W$) to East ($5^\circ W$), observed in the annual signal of the heat-content (Fig. 9), suggests that a major baroclinic event affects the equatorial thermocline on a seasonal time-scale. But phase-speed is about 30 cm/sec, and nearly an order of magnitude less than the first baroclinic Kelvin-wave speed (Merle, 1980). Nevertheless, this observation could be related to the tentative explanation of the seasonal upwelling of the Gulf of Guinea by remote atmospheric forcing and Kelvin-wave guide effect of the equator. Moore *et al.* (1978) have suggested such a mechanism, and O'Brien, Adamec and Moore (1978):

Adamec and O'Brien (1978) offered a Kelvin-wave model of the equatorial Atlantic similar to the one proposed by MacCreary (1976) to explain the Pacific "El Niño" as a response of the Eastern equatorial basin to a remote release of the trade-wind forcing in the Western Pacific. The data processed in this study do not allow us to confirm this particular model.

But we can conclude that in the tropical Atlantic, the depth of the thermocline is changing over a large range on a seasonal time-scale, giving a seasonal variation of heat-storage much larger than the seasonal variation of the net, local heat-gain through the surface. So, a huge redistribution of heat by oceanic motions is occurring. This large oceanic heat-transport at low latitudes, can explain some curious features of the oceanic heat-balance in the Tropics, noticed by Oort and Vonder Haar (1976), like the large seasonal cross-equatorial heat-flux, and the

out of phase in the annual signal of heat-storage (Fig. 1). This out of phase is also observed in the Atlantic Ocean (Fig. 14).

Thus, historical data in the Tropical Atlantic demonstrate that in the vicinity of the equator:

- oceanic advection is the major process of the heat-budget, and cannot be neglected in the models of mixed layer and thermocline;
- a large baroclinic event guided by the equator appears on a seasonal time-scale.

Acknowledgements

This study was partly supported by NSF contract ATM 78-25396, "Climate and heat-transport by the subtropical gyres", as part of the CIMAS activity.

REFERENCES

- Adamec D., O'Brien J. J., 1978. The seasonal upwelling in the Gulf of Guinea due to remote forcing, *J. Phys. Oceanogr.*, **8**, 6, 1050-1060.
- Bryan K., 1962. Measurements of meridional heat-transport by ocean currents, *J. Geophys. Res.*, **67**, 9, 3403-3414.
- Budyko M. I., 1956. *The heat-balance of the Earth's surface*, English translation by US Weather Bureau, Washington D.C.
- Bunker F., Worthington L. V., 1976. Energy exchange charts of the North Atlantic Ocean, *Bull. Am. Meteorol. Soc.*, **57**, 6, 670-678.
- Emig M., 1967. Heat-transport by ocean currents, *J. Geophys. Res.*, **72**, 10, 2519-2529.
- Hastenrath S., 1977. Relative rôle of atmosphere and ocean in the global heat budget: Tropical Atlantic and Eastern Pacific, *Q.J.R. Meteorol. Soc.*, **1**, 3, 519-526.
- Hastenrath S., Lamb P. J., 1978. *Heat-budget Atlas of the Tropical Atlantic and Eastern Pacific Ocean*, The University Wisconsin Press, 140 p.
- Hisard P., Merle J., 1979. Onset of summer surface cooling in the Gulf of Guinea during GATE, *Deep-Sea Res.*, GATE, Suppl. II to V, **26**, 325-342.
- Lamb P., 1978. Case studies of the Tropical Atlantic surface circulation patterns during recent sub-Saharan weather anomalies: 1967 and 1968, *Mon. Weather Rev.*, **106**, 4, 462-491.
- MacCreary J., 1976. Eastern tropical ocean response to changing wind systems; with application to El Niño, *J. Phys. Oceanogr.*, **6**, 5, 632-645.
- Merle J., 1978. Atlas hydrologique saisonnier de l'océan Atlantique intertropical, *Trav. Doc. ORSTOM*, n° 82, 184 p., 8 fig., 153 cartes.
- Merle J., 1980. Seasonal heat-budget in the equatorial Atlantic Ocean, *J. Phys. Oceanogr.*, **10**, 3, 464-469.
- Merle J., Le Floch' J., 1978. Variations saisonnières de la température dans l'Océan Atlantique intertropical, *Oceanol. Acta*, **1**, 3, 271-276.
- Merle J., Fieux M., Hisard P., 1979. Annual signal and interannual anomalies of sea-surface temperatures in the Eastern equatorial Atlantic Ocean, *Deep-Sea Res.*, GATE, Suppl. II to V, **26**, 77-102.
- Moore D. W., Hisard P., McCreary J., Merle J., O'Brien J. J., Picaut J., Verstraete J. M., Wunsch C., 1978. Equatorial adjustment in the Eastern Atlantic, *Geophys. Res. Letters*, **5**, 8, 637-640.
- O'Brien J. J., Adamec D., Moore D. W., 1978. A simple model of equatorial upwelling in the Gulf of Guinea, *Geophys. Res. Lett.*, **5**, 8, 633-636.
- Oort A., Vonder Haar T. H., 1976. On the observed annual cycle in the ocean-atmosphere heat balance over the Northern hemisphere, *J. Phys. Oceanogr.*, **6**, 6, 781-800.
- Sverdrup H. U., 1957. Oceanography, in: *Handbuch der Physik*, **48**, 608-670.
- Vonder Haar T. H., Oort A. H., 1973. New estimate of annual poleward energy transport by Northern hemisphere oceans, *J. Phys. Oceanogr.*, **3**, 169-172.